Precambrian animal diversity: Putative phosphatized embryos from the Doushantuo Formation of China

Jun-Yuan Chen*†‡, Paola Oliveri†§, Chia-Wei Li¶, Gui-Qing Zhou*, Feng Gao*, James W. Hagadorn‖, Kevin J. Peterson§, and Eric H. Davidson‡§

*Nanjing Institute of Geology and Paleontology, Nanjing 210008, China; Divisions of §Biology and ‖Geological and Planetary Sciences, California Institute of Technology, Pasadena, CA 91125; and ¶Department of Life Sciences, National Tsing Hua University, Hsinchu 300, Taiwan, China

Contributed by Eric H. Davidson, January 28, 2000

Putative fossil embryos and larvae from the Precambrian phosphorite rocks of the Doushantuo Formation in Southwest China have been examined in thin section by bright field and polarized light microscopy. Although we cannot completely exclude a nonbiological or nonmetazoan origin, we identified what appear to be modern cnidarian developmental stages, including both anthozoan planula larvae and hydrozoan embryos. Most importantly, the sections contain a variety of small (≤200 μm) structures that greatly resemble gastrula stage embryos of modern bilaterian forms.

The prediction that stem-group and perhaps even crown-group bilaterians existed in Neoproterozoic times, well before the Precambrian boundary, is supported by many kinds of argument. The most general and important of these arguments is that almost all major bilaterian clades already are represented in the Lower Cambrian, in remarkably preserved deposits such as the Chengjiang fossil lagerstätte (1). Fossil remains of diverse bilaterian forms from the Lower Cambrian have been obtained from many other regions of the globe as well (2–4). The latest Precambrian also has yielded trace fossils of unmistakable bilaterian origin (5–7). These remains indicate that major evolutionary diversification of animals already had occurred by the onset of the Cambrian, and, therefore, more remote ancestral forms must have been alive earlier. Cladistic analyses, both morphological and molecular, clearly indicate that the bilaterians are monophyletic, i.e., they derive from a latest common ancestor that gave rise only to bilaterians (see ref. 8). How deep in time were this common ancestor and its offshoots, the common ancestors of the three great bilaterian clades (ecdysozoans, lophotrochozoans, deuterostomes; refs. 8–10) is unknown. Molecular phylogenies based on sequence comparisons of protein domains shared by all bilaterians suggest that the time of divergence of these proteins may extend back to 600–1,200 million years (megaannuum; Ma) ago (11–16). In addition, arguments based on regulatory evolution lead to the proposition that microfaunal bilaterian stem groups must have evolved through several stages of regulatory complexity during Precambrian time (17, 18). But thus far, unequivocal paleontological evidence of bilaterian forms has extended only to the final period of the Neoproterozoic, a few million years before the Cambrian "explosion" (5–7, 19, 20).

The Lower Cambrian strata of Southwest China overlie phosphate deposits known as the Meishucun Formation (Fm), which contains small shelly fossils mainly composed of mineralized spines and plates of various types of animal (21, 22). The Late Precambrian is represented by a thick sequence of carbonate deposits, the Dengying Fm. The top of the Dengying Fm contains the tubular fossil *Cloudina* (19). Below these fossils are frondose Ediacaran remains (23), the affinities of which are enigmatic (24, 25). What has been missing is evidence of animals belonging to the bilaterian lineage deeper in time, i.e., from the Lower Dengying, or from earlier deposits anywhere in the world. One such deposit is the phosphatic Doushantuo Fm, which underlies the Dengying Fm in Southwest China. We report here a preliminary exploration of embryonic and larval animal forms represented in samples of Doushantuo phosphorites from one particular location.

The terminal Proterozoic follows the most recent phase of the worldwide Varanger glaciation, and it extends to the Precambrian/Cambrian boundary at 543 Ma (5, 30). In Hubei and Guizhou provinces of China, the latest Varanger glaciation event is represented by the Nantuo tillites (31). The tillites are believed to have an age of 610–590 Ma (32), and a U-Pb radiometric date suggests a greater age for the underlying formation (33). The Doushantuo Fm lies immediately above the Nantuo Fm, representing transgressive deposits that occurred as the result of a rise in sea level because of the melting of continental glaciers. The time gap between the end of the glaciation and the beginning of transgressive deposition is of unknown length, except that it is certainly younger than the 610- to 590-Ma-old Nantuo tillites. The age of the Doushantuo Fm could be as old as 580 Ma (26), and pending direct measurement, its age must fall within the range 570 ± 20 Ma (27) [Saylor *et al.* (34) argue that it is toward the younger end of this range]. It is important to stress, however, that whatever the absolute time horizon represented by the Doushantuo Fm, it is likely to precede the lowest strata with which bilaterian remains have so far been associated (20).

The Doushantuo Fm is a marine deposit containing phosphate-dolomite sequences. In Beidoushan, in the Weng'an district of central Guizhou Province (Fig. 1), the phosphate deposit is divided by an erosive surface into two units. The fossils described here are from the base of the upper phosphate unit, 0.2–6 m in thickness. This high-resolution fossil bed is about 30% phosphate, present as the mineral fluorapatite [$Ca_5(PO_4)_3F$]. Phosphatic beds within this deposit are grainstones composed of 1- to 5-mm phosphoclasts. These derive from a phosphatic surface that formed on the sea floor, in the process recrystallizing existing surface sediments. In addition to replacing carbonate sediments, soft tissues of metazoan embryos, larvae, adults, and algae also appear to have been mineralized (26–29). The phosphatized sediment crust was then broken into small fragments by heavy current activity and then redeposited and mixed in with adjacent lime muds. For current discussion of this fossilization process, see ref. 28.

Methods

The samples included in the present study were collected from the Wusi and Baidoushan quarries of the Weng'an phosphate mine. Thin sections were prepared by grinding and were mounted on standard microscope slides for examination. Section thickness was 30–50 μm, allowing for some three-dimensional visualization at different planes of focus. About 2,000 sections have been examined, and over 4,000 digital images of embryos and larvae have been recorded. These images were obtained by transmitted light microscopy at ×100 or ×200 magnification, and many samples also were photographed. Selected samples

Abbreviations: Ma, Megaannuum (i.e., million years); Fm, Formation.

†J.-Y.C. and P.O. contributed equally to this work.

‡To whom reprint requests should be addressed at: Division of Biology 156-29, California Institute of Technology, Pasadena, CA 91125. E-mail: davidson@mirsky.caltech.edu; or Nanjing Institute of Geology and Paleontology, Nanjing 21008, China. E-mail: chenjy@jlonline.com.

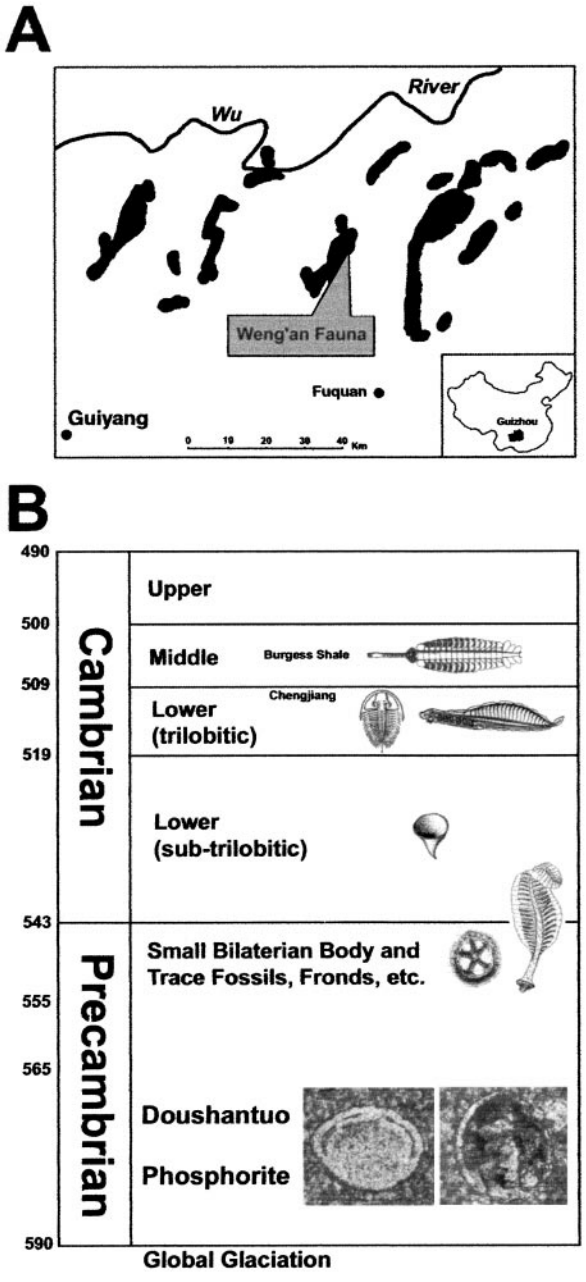

Fig. 1. Locality map and relative generalized stratigraphy of the Doushantuo Fm. (*A*) Location of the Weng'an phosphorite deposits in Guizhou Province, China. Outcrops of the Doushantuo Fm are shown by the black areas. (*B*) Relative stratigraphy of the Terminal Proterozoic and Cambrian. The Doushantuo Fm is older than the late Neoproterozoic paleocommunity Zone III, which bears fossil evidence of cnidarian as well as bilaterian forms. Sponges are clearly present in Precambrian deposits (41, 42), including the Doushantuo (26). Beneath the Doushantuo Fm is a layer of tillite, deposited during the global glaciation, which is believed to have terminated about 590 Ma ago. On the left are interpolated absolute dates; the solid horizontal lines represent divisions dated by U-Pb geochronology. Also indicated are representative Cambrian lagerstätten. The dates shown for the Cambrian are from Landing *et al.* (43, 44) and Davidek *et al.* (45); the Precambrian/Cambrian boundary date is from Bowring *et al.* (30) and Grotzinger *et al.* (5). See text for discussion and references. The fossils shown are, from top to bottom: *Opabinia*, a middle Cambrian Burgess Shale arthropod; a Lower Cambrian olenellid trilobite (left) and *Haikouella lanceolata* (46), an early Cambrian chordate (right); a small shelly fossil of the Lower Cambrian; *Arkarua*, a possible Precambrian echinoderm (left) and a sea pen, *Charniodiscus*, from the later Precambrian (right); a possible sponge embryo from the Precambrian Doushantuo Fm (left), and a fossil embryo resembling a deuterostome gastrula (right; for more details see Fig. 3*A*).

were examined as well in a polarization microscope using cross-polarized light with a gypsum plate.

Apparent Fossil Embryos and Their Affinities with Modern Forms. Each of the forms we report in the following was encountered multiple times. The sections are heterogeneous: some are rich with apparent fossil embryos and/or microscopic sponges in various stages of development, whereas others are devoid of any specimens of interest. The object of this paper is to report the presence of diverse microscopic structures, which, at high resolution, resemble several modern forms of cnidarian larvae (Fig. 2); and most importantly, gastrula stage embryos that appear bilaterian in their morphological details (Fig. 3). We are aware that microscopic mineral inclusions of nonbiological origin can easily resemble biological forms, including embryos, and we cannot rigidly exclude the possibility that they are not fossils at all. However, we consider two kinds of evidence that point instead to a biogenic origin for these embryo-like structures: first and most important, the remarkable consistency of their morphology and dimensions as observed in multiple independent observations of each of the types that we describe; and second, their appearance under polarized light, which allows direct visualization of the crystal structure. Each individual crystal element, defined by the orientation of its axes with respect to the plane of polarization, is displayed in the polarization microscope images by a different color. As we summarize in *Discussion*, the results of the polarized and bright-field microscopy are consistent with the argument that the objects described in Figs. 2 and 3 are indeed fossilized embryos, which originally were composed of epithelial layers of cells surrounding internal cellular structures that arose by invagination.

Possible Cnidarian Gastrulae. Fig. 2*A* shows a form strikingly similar to an early anthozoan planula. The key characteristics, as illustrated in the drawing in Fig. 2*B*, are its elongate shape, in the fossil about 320×220 μm; its single cell-thick ectodermal wall, which can be seen clearly in the portion of the fossil at 9 o'clock, and the multipolar endodermal ingressions protruding into the blastocoel from a cell layer applied to the inner surface of the ectoderm. The double-layered structure is clearly evident in the fossil (at about 7–11 o'clock and at about 5 o'clock on its circumference). Fig. 2 *C* and *D* shows a fossil that displays a unique morphology found in some modern hydrozoan gastrula-stage embryos. These embryos consist essentially of a single cell-thick ectoderm and a thin-walled archenteron also composed of a single cell-thick epithelium (Fig. 2*E*). The polarized light image in Fig. 2*D* reveals the same features; therefore, the crystal elements of which the structural elements we interpret as ectodermal and archenteron walls are composed do not extend beyond the limits visible in white light (i.e., they are not merely color discontinuities in a solid mineral grain). The blastocoelar space and the lumen of the archenteron are amorphous, rather than crystalline, because they appear black in polarized light however the prisms are set. A pink mass at the bottom of the archenteron visible in polarized light appears to be an adventitious grain. A striking feature of this putative fossil embryo is that individual cells can be discerned in many regions of both the ectodermal and endodermal layers, and, in Fig. 2*D* (at about 3–4 o'clock on the perimeter), each cell can be seen to be a separate crystal of a different color from its neighbor. Elsewhere, contiguous cells are represented by crystals oriented in the same direction, perhaps reflecting the original apical-basal orientation of the cytoskeletons in the contiguous cells of the original epithelial wall. This interpretation is enhanced by the observation that the orientations of the crystals in the inner and outer layers in Fig. 2*D* are the same (arrows), as would have been the apical-basal orientation of these cell layers in life.

Possible Bilaterian Gastrulae. Fig. 3 shows a remarkable series of what appear to be fossil embryos that display specific characteristics

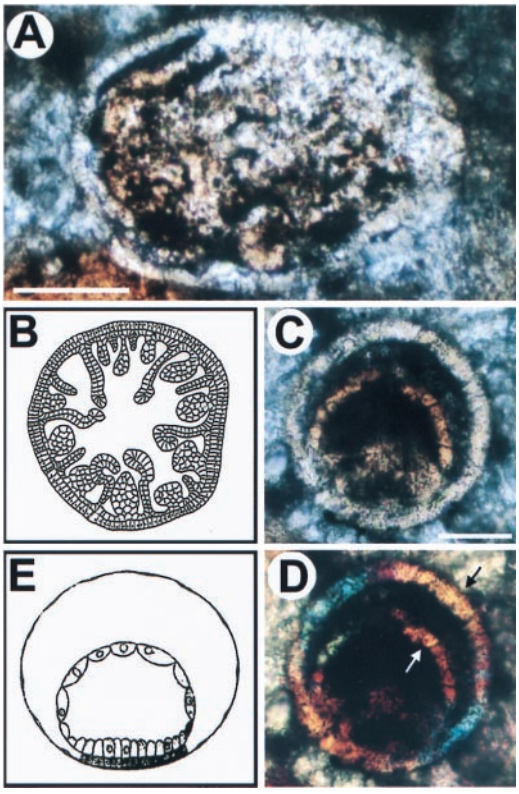

Fig. 2. Putative cnidarian embryos and larvae. (*A*) Oblique section of a possible fossil anthozoan planula. (*B*) Schematic view of a transverse section of the late planula of the anthozoan *Euphyllia rugosa*. The larval stage represented in *A* and *B* is constituted of an outer monocellular layer, the ectoderm, within which is an inner endodermal layer with various mesenteric folds and immature septa. This complicated bilayered structure is typical of anthozoan late planula larvae. Note the individual cells visible in the ectodermal layer at lower left in *A*, where it has separated from the endodermal layer. (Scale bar, 100 μm.) (*C* and *D*) Putative fossil gastrula of hydrozoan medusa; (*C*) Bright field; (*D*) Polarized light. Under polarized light (*D*), both layers show the same crystal orientation at arrows, as indicated by the same colors. The modern hydrozoan embryo shown in *E* is *Liriope mucronata*. *B* is from Chevalier (47); *E* from Campbell (48). (Scale bar in *C* is 50 μm.)

of modern bilaterian gastrula-stage embryos, specifically those of many phyla of modern marine invertebrates. Note first that these are all rather small forms, typically 150–200 μm in diameter, similar to many echinoderm and hemichordate embryos, and to molluscan, polychaete, and a good many other lophotrochozoan embryos. The structures shown in Fig. 3 *A–G* resemble embryos of the echinoderm-hemichordate clade of the deuterostomes, as illustrated by the sea urchin example in Fig. 3*H*. They appear to consist of a single cell-thick ectodermal wall, the organization of which can be clearly seen in the polarized light images of Fig. 3 *B–F*; a large blastocoel; and an archenteron protruding into the blastocoel from one side, which is the location of the blastopore. A further and very particular characteristic is a bilateral endomesodermal outpocketing at the top of the archenteron. Endomesodermal outpockets appear to be present in the specimen shown in Fig. 3*A*, in which the archenteron bends toward one side of the ectoderm. In modern embryos of these kinds, the mouth forms from a columnar ectodermal region where the archenteron contacts the blastocoel wall. Some of these same features are evident in Fig. 3 *C* and *D*, which can be interpreted as an oblique section along the plane similar to that indicated by the arrowheads for the specimen shown in Fig. 3*A*. This plane passes through the tip of what appears to be the archenteron, from which two masses of cells can be seen emerging, adjacent to a thickened region of the blastocoel wall. Note that each of these cells contains a central discontinuity that is in the right position to represent its nucleus. A further example is shown in Fig. 3*E*, although in this specimen a large crystalline mass appearing pink in polarized light (Fig. 3*F*) partially occludes the putative archenteron. However, the single cell-thick wall of the archenteron-like structure can be seen in blue on one side, as can a few blue crystal elements within the blastocoel that could represent individual mesenchymal cells. What seems to be a large blastocoel is particularly evident in Fig. 3*G*. The apparent blastocoelar spaces in the fossil embryos shown in Fig. 3 *A–G* are either entirely amorphous, as in Fig. 3 *C*, *D*, and *G*, or are partially occupied with crystals that are separate from those of the cellular layers, as can be seen in Fig. 3 *B* and *F*. Fig. 3 *I* and *J* shows what could be different forms of fossil gastrulae. These display more of a spiralian character, illustrated by the drawings of polychaete embryos shown in Fig. 3*K*. Gastrula-stage embryos of many marine annelids, molluscs, and their allies are built of larger cells (i.e., at gastrula stage they are composed of fewer cells than are typical deuterostome gastrulae). The archenteron is generated by more or less yolk-filled blastomeres, which, after being surrounded by ectodermal cells, hollow out to form the lumen of the embryonic gut. A particular structural feature of such gastrulae are the bilateral bands of cells originating at one side of the base of the archenteron. These are the mesodermal germ bands. An early stage of germ band formation is illustrated in Fig. 3*K*, and a topologically similar morphological structure is evident in Fig. 3*J*. What appear to be large individual cells can be seen to constitute the ectodermal wall, as well as the archenteron, and between them, on the right, is an additional band of cells extending vertically across the blastocoel. The specimen in Fig. 3*I* is similar in its large and thick archenteron, but the outer wall is thinner than in Fig. 3*J*.

We want to stress that we make no claim that organisms we would recognize as polychaetes or echinoderms existed at the time the Doushantuo sediments were deposited. The comparisons with modern forms in Fig. 3 are intended only to show that the morphological characters of the fossil gastrulae are paralleled in detail by those of modern bilaterian gastrulae. Furthermore, to accommodate the diversity of the fossil gastrulae both deuterostome and spiralian models appear to be required.

Similar Dimensions of Specimens of Each Morphological Form of Putative Microfossil. The internal and external dimensions of several examples, of the much larger number seen, of each of the morphotypes included in Figs. 2 and 3 were measured. A more extensive set of morphometric measurements will be forthcoming, but the data in Table 1 suffice to illustrate the point: considering the complexity of the mineralization process, the dimensional consistency of each type is fairly remarkable. For example, the fraction of the average external diameter constituted by the diameter of the archenteron in the three deuterostome embryo-like specimens is $27 \pm 3\%$, and the thickness of both the apparent endodermal inner layer, and the average thickness of outer wall in all of the cnidarian-like embryos, were always the same.

Discussion

The claim made in this paper is that organisms that produced embryos of bilaterian affinity, as well as clearly differentiated cnidarian forms, may have existed some millions of years earlier than indicated by any previous paleontological evidence. Thus, it is a first order of business to review the evidence that the objects displayed in Figs. 2–4 are likely to be fossil embryos, rather than microscopic spheroidal grains of nonbiological origin.

Qualitative Morphological Evidence of Authenticity. An essential feature of the fossils is their high morphological resolution. This might seem fantastic, had it not already been reported by Li *et al.* (26) in their observations of sponge embryos and by Xunlai and Hofmann (29) in studies of algal and fungal microfossils in sections prepared from the same location. Details of cell nuclei, spicules, fungal mycelia, and subcellular morphology, as well as cells of

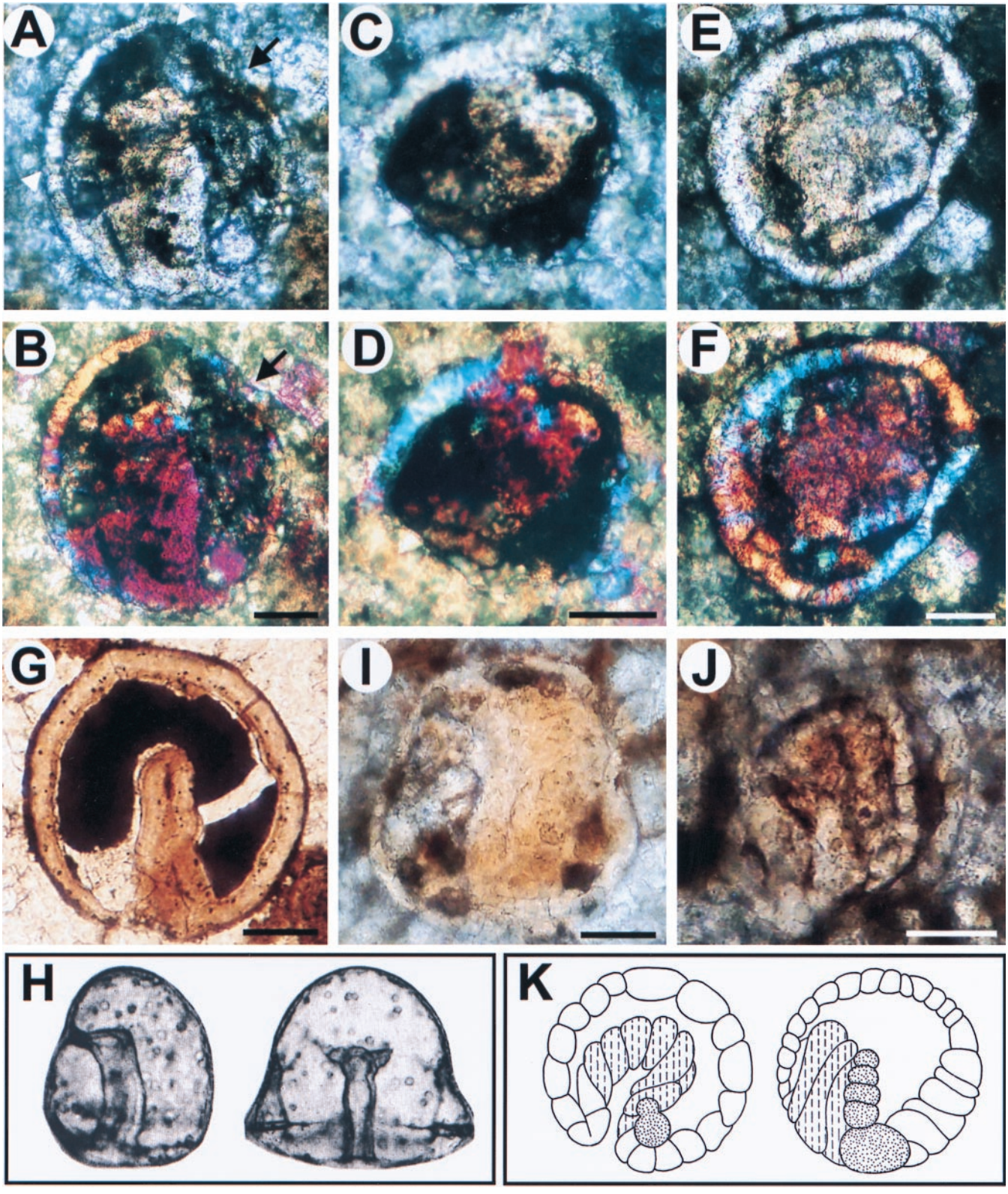

Fig. 3. Putative fossil embryos that resemble bilaterian gastrulae. (*A*–*G*) Fossils resembling deuterostome embryos; (*H*) Modern example (gastrulae of the sea urchin *Mespilia globulus*, ref. 49) In *A*, *C*, and *E*, the archenteron is bent to one side, and in *A* and *C* displays bilobed outpocketings; (*A*) The nearer ectodermal layer is thicker compared with the opposite one (possible oral and aboral ectoderms, respectively; compare *H*). (*C*) A section in the plane indicated by the small arrowheads in *A*. (*B* and *D*) Polarized light microscope images, showing that the cells comprising the outpocketings are differently oriented, as they appear in different colors from those constituting the walls of the gut. In *A*, part of the outer wall is deformed (arrow) by a crystal grain visible in *B* (light pink). (*G*), Another specimen displaying invaginating archenteron at early midgastrula stage. (*H*) Modern sea urchin gastrulae (49). (*I* and *J*), Fossils resembling modern spiralian gastrulae; (*K*) Modern polychaete embryos in which the dashed lines indicate yolky endoderm cells and dots represent mesoderm cells (*Eupomatus*, left; *Scoloplos*, right, redrawn from Anderson, ref. 50). In the fossils *I* and *J*, the archenteron is thick-walled (*cf.* cross section in *C*), and in *J* all of the cells in the embryo, including the ectodermal wall, are conspicuously larger relative to the size of the embryo. Note also the column of cells along the archenteron in *J*. (Scale bars represent 50 μm.)

Table 1. Dimensions (μm) of putative fossil embryos of distinct morphotypes

Type structure	External dimensions	Outer wall	Inner wall(s)	Archenteron diameter
Fig. 2*A*	234 × 333	13.4	9.0*	—
	207 × 252	13.5	—	—
	234 × 234	13.5	9.0*	—
	252 × 297	9.0	9.0*	—
Fig. 2*C*	140 × 140	13.4	6.7	—
	126 × 142	13.4	8.0	—
	135 × 144	13.5; 18†	9.0	—
Fig. 3*A*	196 × 228	16.1§	—	64
Fig. 3*C*	—‡	16.2	—	52
Fig. 3*E*	185 × 202	13.4	—	54
Fig. 3*G*	189 × 197	18.0	—	46
	207 × 234	18.0	—	—
Fig. 3*I*	177 × 181	13.0	—	75, 101†
	162 × 193	13.5, 22.5†	—	112
	180 × 180	18.0	—	90
Fig. 3*J*	131 × 137	18.0	—	78
	144 × 153	10.0	—	63

Measurements were taken from photographic representations of sections and converted to μm by reference to size standards. Short horizontal lines denote features not relevant to specimen, or occluded, or otherwise impossible to measure.

*Average of several measurements of thickness of wall of multiple in-foldings.

†Different regions of wall of different thickness.

‡External dimensions not comparable because section is oblique and above the equator of the embryo [it measured 134.4 × 147.8; on the embryo shown in *A*, this section (white arrowheads) would have measured 153 μm in diameter].

§The ''oral'' portions of the wall nearest the archenteron were measured.

various sizes, can be seen in these works [sponge embryos similar in every respect to those described (26) were frequently encountered in the same slides that included the fossil embryos discussed here]. Thus, if the putative cnidarian and bilaterian fossils are authentic, their morphological features should be visible on the same fine scale, and indeed they are. Many very specific morphological characters of modern gastrula-stage cnidarian and bilaterian forms can be seen: The structures appear to be bounded by single cell-thick walls that enclose blastocoelar spaces of familiar dimension; the bilaterian-like forms display archenterons; and the cnidarian-like forms other typical endodermal morphologies. Each of the types we have categorized in Figs. 2 and 3 have been seen multiple times in the sections examined. Furthermore, as Table 1 illustrates, the dimensions of each type are always approximately the same. Constant morphology and constant dimension are the outputs of genetically controlled developmental systems and are thus a powerful index of biological origin.

It would have been suspicious had every embryo we encountered seemed to display affinity with some modern taxon. But such was not the case. Various forms that we saw cannot immediately be identified by similarity to modern models, and an example is shown in Fig. 4*D*; its affinities are problematic.

Physical Evidence. The polarized and bright-field image pairs shown in Fig. 2 *C* and *D* and Fig. 3 *C–H* provide additional evidence. Although oncoids occur in these sections (although quite rarely, compared with fossil embryos), their concentric, often laminar structures appear quite different from those of the putative fossil embryos when viewed in polarized light. Examples of oncoids found in the sections we studied are shown in Fig. 4 *A–C*. Fig. 4 *A* and *B* illustrates an initial stage of concentric lamination around a phosphatic nucleus. These coated grains are dissimilar to one another in size, crystal structure, number of laminations, and lamination thickness. The main feature of the polarized and bright-field image pairs in Figs. 2 and 3 is that the morphology of the putative fossil embryos looks the same by either display. Therefore, the boundaries of the crystal domains detected in polarized light are also the morphological boundaries of the structures seen in the light microscope: the blastocoels are real, rather than simply discolored crystal boundaries; the apparent single cell-thick walls that bound the embryos are discontinuous with the external matrix in which they are embedded, as well as with the amorphous material in the blastocoelar spaces; the same can be said for the structures resembling archenterons, which are so important a diagnostic feature for the bilaterian embryos. Additional features visible in polarized light are noted above that demonstrate authenticity in unexpected specific ways. In Fig. 2*D*, for example, the orientations of the crystals in what look to be the endodermal and ectodermal cell layers of the embryo are in several places the same, as indicated by the similar colors (arrows). This similarity might be expected, because the apical-basal orientation of the cells of which this embryo was composed should have been the same in both layers. Perhaps the apical-basal orientation of some aspect of internal cytoarchitecture was reflected in the formation of the initial mineral substituent within these cells. In several of the images, individual contiguous cells appear to have been reconstituted as individual crystals, seen in polarized light in different colors, because their axes are noncoincident (Figs. 2*F*, 3*D*, and 4*F*). Throughout most of the polarized light images, large contiguous patches of cells constituting a given epithelial layer generally display the same crystal orientation. In Fig. 3 *A* and *B*, we can see that the original structure from which the fossil formed was soft, for its external wall is deformed by a hard grain against which it still lies (arrow).

Although the physical and biological evidence both support the

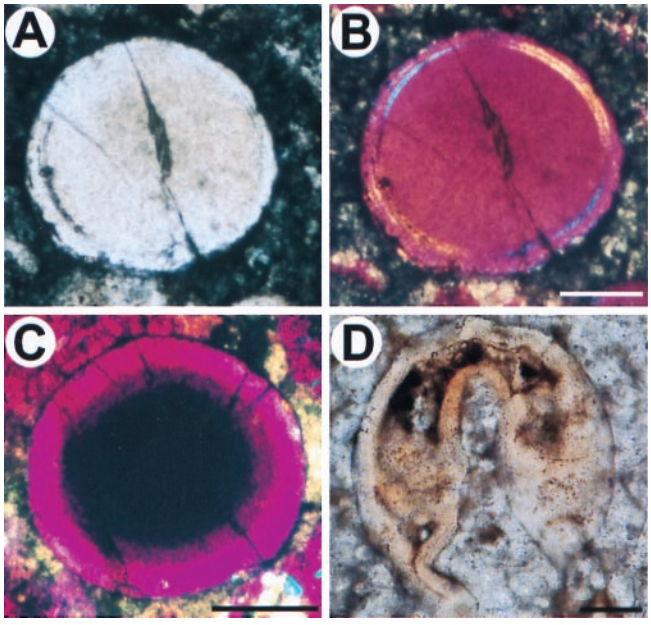

Fig. 4. Oncoids and an undefined embryo, larva, or adult form. Bright-field (*A*) and polarized (*B*) light images of an oncoid found in one of the thin sections. The inner mass consists of a unique homogeneous crystal, as shown by its uniform color in polarized light, surrounded by a laminar structure. Note the crack in the center. The two outside thin layers are uniform, and they do not delimit any cavity. (*C*) A smaller oncoid; note the uniform circumferential wall, which in polarized light is the same color throughout. (*D*) Unidentified biological form. There is a large blastocoel and a gut of some kind. The top of the fossil embryo is slightly deformed, suggesting that this structure was soft. (Scale bars are 50 μm.)

authenticity of the fossil embryos, it remains formally possible that only some aspects of the fossils are biogenic (perhaps not even metazoan), whereas other features of their structures are nonbiogenic. However, we think the initial evidence presented here implies that embryos of diverse metazoan affinity were in fact present several tens of millions of years before the onset of the Cambrian. At the very least, it is clear that the Doushantuo microfossils must be considered a very important subject for further study.

The Putative Bilaterian Embryos. In deuterostomes of the hemichordate/echinoderm clade, the large blastocoel surrounding the invaginated archenteron is devoid of all but a few mesenchymal cells, whereas in lophotrochozoan protostomes it is more or less filled with large gut cells. The outer wall of the embryo in both groups consists of a single cell-thick ectodermal epithelium. In typical modern echinoderm and hemichordate gastrulae, mesodermal outpocketings emerge from the anterior portion of the gut, whereas in lophotrochozoans the mesoderm arises as columns of cells emerging from bilateral cell masses at either side of the gut. By the time of mesoderm formation, bilateral organization is obvious in both groups. Fig. 3 *B–H* illustrate possible gastrula-stage embryos that appear clearly deuterostome in form; some of these embryos even display apparent mesodermal outpocketings (Fig. 3 *A–D*). The large blastocoel and the characteristic deuterostome archenterons are particularly clear in Fig. 3 *A*, *C*, and *G*. Fig. 3 *I* and *J* shows apparent fossil gastrulae that, in their large cells and relatively thick archenterons, instead appear spiralian. These assignments are of course tentative, but we note that, were it the case that these are indeed embryos of spiralian affinity, this would imply that crown-group bilaterians had already diversified (35) and that the stem groups lie much deeper in time. In any case, assuming that they are indeed real, the bilaterian nature of the fossil embryos in Fig. 3 is hard to doubt. The present report is to be considered an initial analysis, in that the actual diversity of bilaterian forms in the Doushantuo phosphorites can be established only by examination of later developmental stages, if they can be recovered. But on molecular and phylogenetic as well as paleontological bases, it is already likely that the bilaterians have an evolutionary history that long precedes the Ediacaran, let alone the Cambrian "explosion."

Indirect Development. If the Precambrian embryonic organisms of bilaterian form discussed here developed into organisms that we could recognize as similar to adult bilaterian forms, they almost certainly did so indirectly, using planktotrophic larval forms. This is a safe inference from the small size and the morphology of these embryos, which resemble those of indirectly developing deuterostomes (i.e., echinoderms or hemichordates) or spiralians (e.g., the polychaete embryos of the models in Fig. 3*K*). Most directly developing marine bilaterians use much larger eggs that are able to produce embryos consisting of relatively large numbers of cells without feeding. Many lines of evidence show that for deuterostomes and lophotrochozoans maximal indirect development is primitive, and direct development is derived (36–38). A palentological argument against this view has been cited (39) based on some large eggs of Cambrian origin (40). However, there is so far no evidence of embryos of bilaterian nature in the Doushantuo phosphorites that are more than 250 μm in diameter, or that have forms which support the possibility of direct development [some frequently occurring, $\geq$500-μm cleavage-stage eggs in the Doushantuo phosphorites (27) are probably of poriferan origin (ref. 26, and our unpublished data)]. Thus, the earliest bilaterian-grade embryos, of which there is only palentological evidence, either produced small and simple creatures compared with modern adult bilaterians, or produced adult bilaterian forms by indirect processes.

Conclusions

This study suggests that the evolutionary history of both cnidarian and bilaterian forms may extend many millions of years deeper in Precambrian time than previous direct evidence so far indicates. But this is only a beginning. Continued exploration of these high-resolution phosphorite deposits may revolutionize palentological insight into the evolutionary origins of animal forms.

We thank the many colleagues in the paleontology and evolution communities who have read, criticized, and thereby vastly improved drafts of this manuscript. This work was supported by the National Science Foundation, China, jointly with the National Department of Science and Technology of China; the National Science Council of Taiwan, China; the Fundamental Biology Research Program of the Life Sciences Division of NASA/Ames, Grant NAG2-1368; and the Norman Chandler Professorship at Caltech. J.W.H. was supported by Fellowships of the Division of Geological and Planetary Science of Caltech, and P.O. was supported by the Stowers Institute for Medical Research.

1. Chen, J.-Y. & Zhou, G.-Q. (1997) in *The Cambrian Explosion and the Fossil Record (Bulletin of the National Museum of Natural Science)*, eds. Chen, J.-Y., Cheng, Y. N. & Iten, H. V. (National Museum of Natural History, Taichung), Vol. 10, pp. 11–105.
2. Bengtson, S., Conway Morris, S., Cooper, B. J., Jell, P. A. & Runnegar, B. N. (1990) *Mem. Ass. Australas. Palaeontols.* **9,** 1–364.
3. Conway Morris, S. & Peel, J. S. (1990) *Nature (London)* **345,** 802–805.
4. Landing, E., Narbonne, G. M., Myrow, P., Benus, A. P. & Anderson, M. M. (1988) in *Trace Fossils, Small Shelly Fossils and the Precambrian/Cambrian Boundary*, eds. Landing, E., Narbonne, G. M. & Myrow, P. (Bulletin of the New York State Museum Number 463, Albany, NY), pp. 18–58.
5. Grotzinger, J. P., Bowring, S. A., Saylor, B. Z. & Kaufman, A. J. (1995) *Science* **270,** 598–604.
6. Fedonkin, M. A. & Wagoner, B. M. (1997) *Nature (London)* **388,** 868–871.
7. Fedonkin, M. A. (1994) in *Early Life on Earth: Nobel Symposium No. 84*, ed. Bengtson, S. (Columbia Univ. Press, New York), pp. 370–388.
8. Adoutte, A. (2000) *Proc. Natl. Acad. Sci. USA* **97,** 4453–4456.
9. Aguinaldo, A. M. A., Turbeville, J. M., Linford, L. S., Rivera, M. C., Garey, J. R., Raff, R. A. & Lake, J. A. (1997) *Nature (London)* **387,** 489–493.
10. Adoutte, A., Balavoine, G., Lartillot, N. & de Rosa, R. (1999) *Trends Genet.* **15,** 104–108.
11. Wray, G. A., Levinton, J. S. & Shapiro, L. H. (1996) *Science* **274,** 568–573.
12. Ayala, F. J., Rzhetsky, A. & Ayala, F. J. (1998) *Proc. Natl. Acad. Sci. USA* **95,** 606–611.
13. Gu, X. (1998) *J. Mol. Evol.* **47,** 369–371.
14. Bromham, L., Rambaut, A., Fortey, R., Cooper, A. & Penny, D. (1998) *Proc. Natl. Acad. Sci. USA* **95,** 12386–12389.
15. Lynch, M. (1999) *Evolution (Lawrence, Kans.)* **53,** 319–325.
16. Wang, D. Y.-C., Kumar, S. & Hedges, S. B. (1999) *Proc. R. Soc. London Ser. B* **266,** 163–171.
17. Davidson, E. H., Peterson, K. J. & Cameron, R. A. (1995) *Science* **270,** 1319–1325.
18. Peterson, K. J. & Davidson, E. H. (2000) *Proc. Natl. Acad. Sci. USA* **97,** 4487–4492.
19. Bengtson, S. & Yue, Z. (1992) *Science* **257,** 367–369.
20. Gehling, J. G., Narbonne, G. M., Jensen, S. & Droser, M. L. (1999) *Geol. Soc. Am. Abstr. Prog.* **31,** 362.
21. Qian, Y., Chen, M. & Chen, Y. (1979) *Acta Paleont. Sinica* **18,** 207–232.
22. Xing, Y., Ding, Q., Luo, H., He, T. & Wang, Y. (1984) *Chin. Acad. Geol. Sci.* **7,** 1–262.
23. Sun, W. (1986) *Precamb. Res.* **31,** 361–375.
24. Seilacher, A. (1989) *Lethaia* **22,** 229–239.
25. Runnegar, B. (1995) *N. Jb. Geol. Palont. Abh.* **195,** 303–318.
26. Li, C.-W., Chen, J.-Y. & Hua, T.-E. (1998) *Science* **279,** 879–882.
27. Xiao, S., Zhang, Y. & Knoll, A. H. (1998) *Nature (London)* **391,** 553–558.
28. Zhang, Y., Yin, L., Xiao, S. & Knoll, A. H. (1998) *Paleont. Soc. Mem.* **50,** 1–52.
29. Xunlai, Y. & Hofmann, H. J. (1998) *Alcheringa* **22,** 189–222.
30. Bowring, S. A., Grotzinger, J. P., Isachsen, C. E., Knoll, A. H., Pelechaty, S. M. & Kolosov, P. (1993) *Science* **261,** 1293–1298.
31. Shields, G. (1999) *Eclogae Geol. Helv.* **92,** 221–233.
32. Knoll, A. H. & Walter, M. R. (1992) *Nature (London)* **356,** 673–678.
33. Zhao, Z., Xing, Y., Ma, G. & Chen, Y. (1985) *Biostratigraphy of the Yangtze Gorge Area, (1) Sinian* (Geological Publishing House, Beijing).
34. Saylor, B. Z., Kaufman, A. J., Grotzinger, J. P. & Urban, F. (1998) *J. Sediment. Res.* **68,** 1223–1235.
35. Valentine, J. W. (1997) *Proc. Natl. Acad. Sci. USA* **94,** 8001–8005.
36. Peterson, K. J., Cameron, R. A. & Davidson, E. H. (1997) *BioEssays* **19,** 623–631.
37. Peterson, K. J., Cameron, R. A. & Davidson, E. H. (2000) *Dev. Biol.* **219,** 1–17.
38. Nielsen, C. (1998) *Biol. Rev. Camb. Philos. Soc.* **73,** 125–155.
39. Conway Morris, S. (1998) *BioEssays* **20,** 676–682.
40. Bengtson, S. & Zhao, Y. (1997) *Science* **277,** 1645–1648.
41. Brasier, M., Green, O. & Shields, G. (1997) *Geology* **25,** 303–306.
42. Gehling, J. G. & Rigby, J. K. (1996) *J. Paleontol.* **70,** 185–195.
43. Landing, E., Bowring, S. A., Fortey, R. A. & Davidek, K. L. (1997) *Can. J. Earth Sci.* **34,** 724–730.
44. Landing, E., Bowring, S. A., Davidek, K. L., Westrop, S. R., Geyer, G. & Heldmaier, W. (1998) *Can. J. Earth Sci.* **35,** 329–338.
45. Davidek, K., Landing, E., Bowring, S. A., Westrop, S. R., Rushton, A. W. A., Fortey, R. A. & Adrain, J. M. (1998) *Geol. Mag.* **135,** 305–309.
46. Chen, J.-Y., Huang, D.-Y. & Li, C. W. (1999) *Nature (London)* **402,** 518–522.
47. Chevalier, J.-P. (1987) in *Traité de Zoologie*, ed. Grassé, P.-P. (Masson, Paris), pp. 403–764.
48. Campbell, R. D. (1974) in *Reproduction of Marine Invertebrates*, ed. Giese, A. C. & Pearse, J. S. (Academic, New York), Vol. 1, pp. 133–199.
49. Okazaki, K. (1975) in *The Sea Urchin Embryo*, ed. Czihak, G. (Springer, Berlin), pp. 177–232.
50. Anderson, D. T. (1973) *Embryology and Phylogeny in Annelids and Arthropods* (Pergamon, Oxford).